

Preparation of Texture Controlled Lead Zirconate Titanate Thick Films with Seed Layer

Takashi Iijima, Sachiko Ito, Hirofumi Matsuda, Masanao Tani*, Masahiro Akamatsu* and Yoshiaki Yasuda*

Smart Structure Research Center, AIST, Tsukuba central 2, 1-1-1 Umewazono, Tsukuba 305-8568, Japan

Fax: 81-29-861-3126, e-mail: iijima-t@aist.go.jp, ¹Research &

²Development Center, Stanley Electric Co., Japan

Preparation of thick lead zirconate titanate (PZT) films with sufficient ferroelectric and piezoelectric properties is required to materialize the piezoelectric a microelectromechanical system (MEMS) devices like micro-actuators and -transducers. An arc-discharged reactive ion-plating (ADRIP) process is one of the candidates to fabricate the thick PZT films because of high deposition rate such as 3 $\mu\text{m}/\text{h}$, but the texture of prepared films shows random orientation. On the other hand, a chemical solution deposition (CSD) process has an advantage to fabricate (100) or (111) preferentially oriented PZT thin films. In this study, the ADRIP derived PZT thick films were deposited onto the 60-nm-thick CSD derived seed layer to control the texture orientation, and 1.6- μm -thick (001)(100) or (111) preferentially oriented PZT films were successfully prepared on Pt/Ti/SiO₂/Si substrates at a high speed deposition rate, 3 $\mu\text{m}/\text{h}$. The texture-controlled thick films showed flat surface and dense microstructure. Moreover, columnar structure was observed for (100) dominant texture. The prepared films showed good ferroelectric and piezoelectric properties. Therefore, integration of CSD and ADRIP process is considered to be texture controlled high-speed deposition technique of PZT thick films for piezoelectric film devices.

Key words: chemical solution deposition, arc-discharged reactive ion plating, PZT, thin film, ferroelectric property

1. INTRODUCTION

Microelectromechanical systems (MEMS) is a effective way to achieve high-performance small device such as acceleration sensors, microactuators, inkjet-printer heads, and ultrasonic motors [1-5]. Ferroelectric lead zirconate titanate (PZT) films are considered to be key material to realize the devices. However, the amount of the displacement and generative force of PZT thin films is not sufficient in some applications of microactuators. To achieve the property of large displacement, increase of the film thickness or improvement of the piezoelectric property is required. One of the techniques to improve the ferroelectric and piezoelectric properties is assumed to be the arrangement of the polarization direction using a texture control process. Various possibilities of the texture control of PZT thin film were investigated for a sol-gel, [6,7] sputtering [8] and MOCVD process [9-11]. Moreover, to increase the amount of displacement and generative force of PZT films, various fabricating processes for PZT thick films on silicon substrates, such as screen printing [12-14], sol-gel [15, 16], hydrothermal [17], gas deposition processes [18], and complex process [19, 20] were reported. From the viewpoint of piezoelectric MEMS devices with the Si micro machining, a low process temperature of texture controlled PZT thick films are required. We consider that a chemical solution deposition (CSD) process is candidate to prepare the texture controlled PZT thick films with dense microstructure at low process temperature, and fabricated

more than 10- μm -thick PZT film using the CSD process. [21] However, a sequence of coating process should be required to increase a film thickness for CSD process, so that it takes long time to prepare thick films. This means a low film deposition rate. Therefore, a high deposition rate process is considered. An arc-discharged reactive ion-plating (ADRIP) process has the advantage of high deposition rate because this process is based on evaporation from metal sources. Furthermore, the plasma density of the arc discharge (10^{12} cm^{-3}) is one thousand times higher than that of the glow discharge (10^9 cm^{-3}) such as sputtering and plasma-enhanced chemical vapor deposition (PCVD). Investigation of ADRIP process for PZT thick films was performed, and high deposition rate, about 3 $\mu\text{m}/\text{h}$, was achieved [22]. However, texture of the prepared PZT thick film showed random orientation. In this study, CSD and ADRIP process were integrated to prepare texture controlled PZT thick films. At first, (100) or (111) preferentially oriented seed layer was prepared on the substrate by CSD process and PZT was grown on the seed layer by ADRIP process.

2. EXPERIMENTAL PROCEDURE

Trihydrated lead acetate (99.9%, Nakarai Tesuque), titanium iso-propoxide (97%, Kanto Chemical) and zirconium n-propoxide (70% in propanol, Gerest Inc.) were used as starting materials, and 2-methoxyethanol (99.7%, Aldrich) was used as a solvent to prepare the CSD precursor solution for seed layer. The nominal compositions of the solutions were equivalent to those of

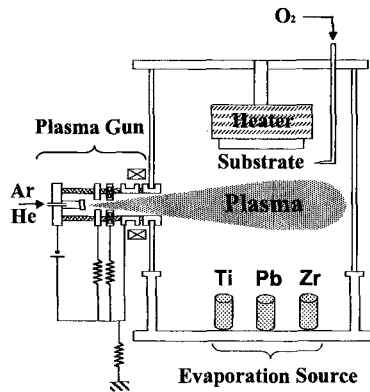


Fig. 1 Schematic illustration of the arc-discharged reactive ion-plating (ADRIP) apparatus.

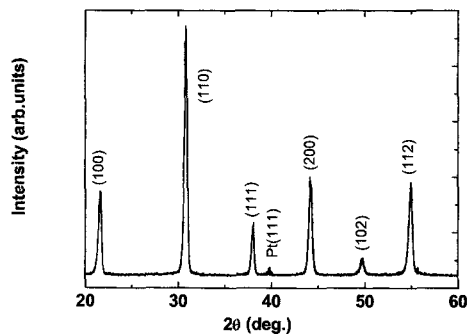


Fig. 2: X-ray diffraction patterns of the PZT film prepared by ADRIP process.

$\text{Pb}_{1.1}(\text{Zr}_{0.53}\text{Ti}_{0.47})\text{O}_3$. Concentration of the Pb-Zr-Ti precursor solution was controlled at 0.5M. To form seed layer, the precursor solution was deposited on a Pt(111)/Ti/SiO₂/Si substrate using a spin coater operating at 3000 rpm for 40 s. The coated samples were dried at room temperature, pyrolyzed at 400-500°C for 3 min, and fired at 700°C for 3 min. Texture orientation of the seed layer was controlled by the pyrolysis temperature. When the pyrolysis temperature is lower than 450, texture show (100) dominant orientation. On the other hand, texture show (111) dominant orientation, when the pyrolysis temperature is higher than 450 [21].

A schematic diagram of this ADRIP apparatus is shown in Fig. 1. The apparatus contains a DC arc-discharged plasma gun and three independent evaporation metal sources, which were Pb (99.9%), Zr (99.9%) and Ti (99.9%). The plasma gun consists of a hot cathode, intermediate grid electrodes, and a ring anode. Rare gases, such as Ar or He, were led into the plasma gun from the cathode. The pressure within the gun could be maintained at approximately 100 Pa using grid orifices. When an appropriate DC bias voltage is applied to the gun, a glow-discharged plasma is generated first, which is then converted to an arc-discharged plasma that expands to the vacuum chamber along a magnetic field generated by a Helmholtz coil. Oxygen was introduced to the chamber as a reactive gas to generate mixed plasma containing a

Table I: PZT films deposition condition of ADRIP process

| | |
|-----------------------|---|
| Source materials | Pb (99.9%), Zr (99.9%), Ti (99.9%) |
| Discharge voltage | 100-200 V |
| Discharge current | 70 A |
| Gas flow rate | O ₂ : 200 sccm, Ar (He): 30 (70) sccm |
| Total pressure | 0.2 Pa |
| Substrate temperature | 500-550°C |
| Deposition rate | 1.9-5.6 μm/h |

large amount of oxygen radicals. The typical deposition conditions are summarized in Table I. The deposition pressure kept to about 0.2 Pa. The Pt(111)/Ti/SiO₂/Si substrates were heated at 500-550°C. The usual PZT film deposition rate was approximately 2-5 μm/h, and the film composition was controlled at approximately $\text{Pb}(\text{Zr}_{0.53}\text{Ti}_{0.47})\text{O}_3$.

The crystal structure of the thin films was examined with an X-ray diffractometer (XRD). The microstructure of the films was observed with scanning electron microscope (SEM, S-5000, Hitachi). An AFM probing system (Nano-R, Toyo Corporation) was connected with a ferroelectric test system (FCE-PZ, Toyo Corporation) to measure *P-E* hysteresis curves and longitudinal displacement-field curves simultaneously with bipolar drive voltages at 5 Hz. The longitudinal displacement of the samples was measured using a PID controlled Z-feedback signal of the AFM conductive cantilever.

3. RESULTS AND DISCUSSION

Figure 2 shows an XRD pattern of a PZT film deposited on to Pt(111)/Ti/SiO₂/Si substrate by ADRIP process. The XRD pattern shows a well-defined perovskite structure, except for the Pt peak, and peaks of pyrochlore phase or any other phases were not observed. Therefore, the prepared PZT film seems to be perovskite single phase. It can be seen that the highest peak is (110) plane, and intensity of the (100) or (111) peaks are not so high. From these results, texture of the ADRIP derived PZT film is considered to show random orientation like PZT powder diffraction pattern.

To control the texture of the films, a PZT seed layer was formed on the Pt(111)/Ti/SiO₂/Si substrate using the CSD process. (100) or (111) preferred 60-nm-thick PZT seed layer was prepared by one coating process, and then PZT film was grown on the seed layer using the ADRIP process. The deposition rate of the ADRIP derived film was 3 μm/h. Figure 3 and 4 shows XRD patterns of the PZT films deposited onto the seed layer. It can be seen that the PZT film grown on (100) dominant seed layer showed strongly (001)(100) preferred orientation. Moreover, texture of the PZT film grown on (111) dominant seed layer was (111) orientation. These results suggest that the seed layer affect the orientation of grown film texture. Figure 5 shows cross section SEM micrograph for (001)(100) dominant oriented PZT film, and Figure 6 shows cross section micrograph for (111) dominant oriented film, respectively. Film thickness of prepared films was 1.6 μm. These microstructures were dense and any defects such as pore cannot be seen. In the

case of (001)(100) preferred oriented film, densely packed columnar grains grew in the region of the bottom electrode and penetrated through the film. On the other hand, the microstructure of (111) dominant oriented film was much different from that of (001)(100) oriented film, because grain structure was complex. Furthermore, it is very difficult to distinguish the interface between the seed layer and growth layer for (100)(001) oriented and

(111) oriented film. This means that the morphology of the PZT films grown by ADRIP process is related to the seed layer and the texture control is possible using the CSD technique, while the texture without seed layer shows random orientation. Therefore, integration of CSD and ADRIP process can achieve texture controlled high-speed deposition of PZT thick films.

Figure 7 shows *P-E* hysteresis curve of texture

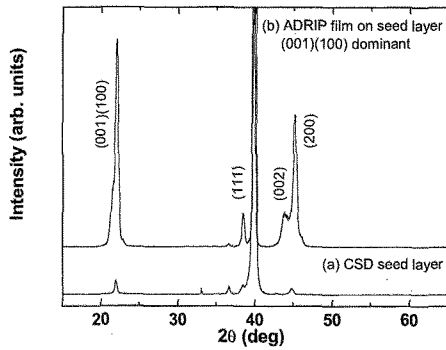


Fig. 3 XRD patterns of the PZT films deposited onto the (100) oriented seed layer.

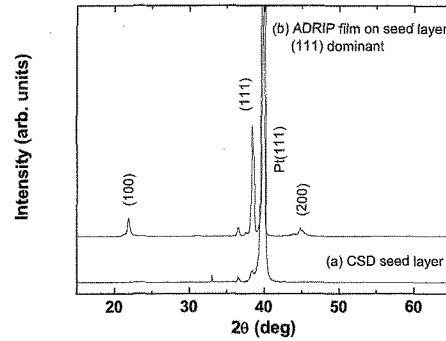


Fig. 4 XRD patterns of the PZT films deposited onto the (111) oriented seed layer.

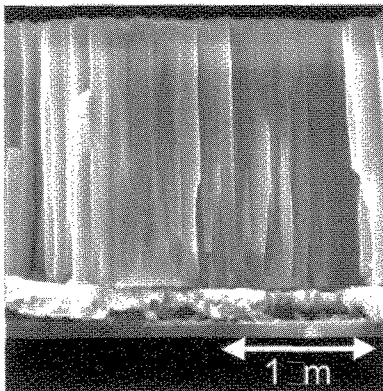


Figure 5 Cross section SEM micrograph of (001)(100) dominant oriented PZT film.

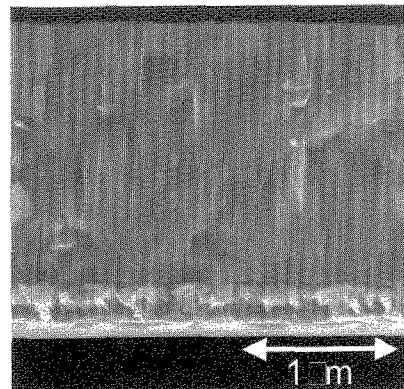


Figure 6 Cross section SEM micrograph of (111) dominant oriented film.

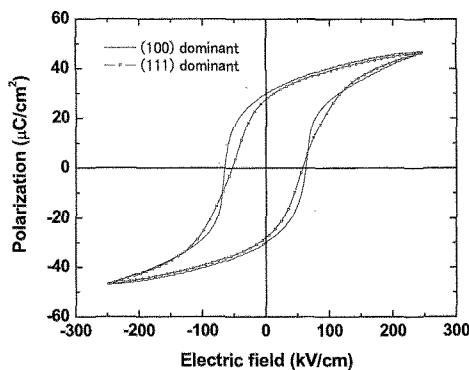


Fig. 7 *P-E* hysteresis curves of (001)(100) and (111) dominant oriented film.

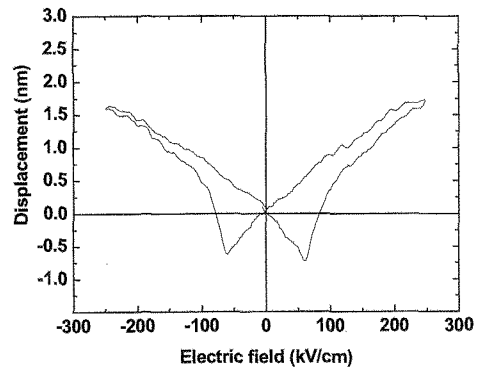


Fig. 8 Longitudinal displacement curve of (001)(100) dominant oriented film.

controlled PZT film prepared by ADRIP process with CSD seed layer. These curves were well saturated so that the prepared films show good ferroelectricity. On the other hand, there is no remarkable difference of the ferroelectric properties between (001)(100) dominant and (111) dominant films. The remnant polarization, P_r , and coercive field, E_c , were $P_r = 30 \mu\text{C}/\text{cm}^2$ and $E_c = 62 \text{kV}/\text{cm}$ for (001)(100) dominant film, and $P_r = 28 \mu\text{C}/\text{cm}^2$ and $E_c = 58 \text{kV}/\text{cm}$ for (111) dominant film. However, the hysteresis rectangularity of (001)(100) dominant film is better than that of (111) dominant film.

Figure 8 shows bipolar driven longitudinal displacement of (001)(100) dominant film measured with AFM. Top electrode diameter was $80 \mu\text{m}$. A typical butterfly-shaped displacement curve related with piezoelectric response was observed. The amount of displacement was about 2nm. Therefore, the texture controlled PZT thick films grown by ADRIP process on the CSD derived seed layer shows piezoelectricity and can be applicable to the piezoelectric film devices.

4. CONCLUSIONS

Texture controlled seed layers were prepared by CSD process, and PZT layers were grown by ADRIP process at a deposition rate of $3 \mu\text{m}/\text{h}$. (001)(100) or (111) oriented $1.6 \mu\text{m}$ -thick PZT were successfully fabricated. The texture-controlled thick films showed flat surface and dens microstructure, and the films showed good ferroelectric and piezoelectric properties. Therefore, integration of CSD and ADRIP process can achieve texture controlled high-speed deposition of PZT thick films for piezoelectric film devices.

REFERENCES

- [1] N Nemirovsky, P. Muralt, N. Setter, and A. Nemirovsky, *Sensors and Actuators A*, **56**, 239-249 (1996).
- [2] S. Wakabayashi, M. Sakata, H. Goto, M. Takeuchi, and T. Yada, *Jpn. J. Appl. Phys.*, **35**, 5012-5014 (1996).
- [3] P. Muralt, A. Kholkin, M. Kohli, and T. Maeder, *Sensors and Actuators A*, **53**, 398-404 (1996).
- [4] M. Hoffmann, T. Leuerer, C. Krueger, U. Boettger, W. Mokwa, and R. Wasser, *Mat. Res. Soc. Symp. Proc.*, S. R. Gilbert, S. T-Mckinstry, Y. Miyasaka, S. K. streiffer, D. J. Wouters, **688**, pp. 145-152, Material Research Society, Warrendale, 2002.
- [5] P. Muralt, M. Kohli, T. Maeder, A. Kholkin, K. Brooks, N. Setter, and R. Luthier, *Sensors and Actuators A*, **48**, 157-165 (1995).
- [6] K. Aoki, Y. Fukuda, K. Numata, and A. Nishimura, *Jpn. J. Appl. Phys.*, **33**, 5155-5158 (1994).
- [7] K. G. Brooks, I. M. Reaney, R. Klissurska, Y. Huang, L. Bursill, and N. Setter, *J. Mater. Res.*, **9**, 2540-2553 (1994).
- [8] M. Adachi, T. Matsuzaki, T. Yamada, T. Shiosaki, and A. Kawabata, *Jpn. J. Appl. Phys.*, **26**, 550-553 (1987).
- [9] Y. Sakashita, T. Ono, H. Segawa, K. Tominaga, and M. Okada, *J. Appl. Phys.*, **69**, 8352-8357 (1991).
- [10] D. Kim, T. Y. Kim, J. K. Lee, W. Tao, and S. B. Desu, *Mat. Res. Soc. Symp. Proc.*, S. B. desu, R. Ramesh, B. A. Tuttle, R. E. Jones, I. K. Yoo, **433**, pp. 213-224, Material Research Society, Pittsburgh, 1996.
- [11] S. Yokoyama, Y. Honda, H. Morioka, T. Oikawa, H. Funakubo, T. Iijima, H. Matsuda, and K. Saito, *Appl. Phys. Lett.*, **83**, 2408-2410 (2003).
- [12] H. D. Chen, K. R. Udayakumar, L. E. Cross, J. J. Bernstein, and L. C. Niles, *J. Appl. Phys.*, **77**, 3349-3353 (1995).
- [13] Y. Akiyama, K. Yamanaka, E. Fujisawa, and Y. Koiwa, *Jpn. J. Appl. Phys.*, **38**, 5524-5527 (1999).
- [14] Y. Jeon, J. Chung, and K. No, *J. Electroceramics*, **4**, 195-199 (2000).
- [15] D. A. Barrow, T. E. Petroff, R. P. Tandon, and M. Sayer, *J. Appl. Phys.*, **81**, 876-881 (1997).
- [16] H. D. Chen, K. R. Udayakumar, C. J. Gaskey, L. E. Cross, J. J. Bernstein, and L. C. Niles, *J. Am. Ceram. Soc.*, **79**, 2189-2192 (1996).
- [17] Y. Ohba, M. Miyauchi, T. Tsurumi, and M. Daimon, *Jpn. J. Appl. Phys.*, **32**, 4095-4098 (1993).
- [18] J. Akedo, and M. Lebedev, *Jpn. J. Appl. Phys.*, **38**, 5397-5401 (1999).
- [19] T. Ohno, M. Kunieda, H. Suzuki, and T. Hayashi, *Jpn. J. Appl. Phys.*, **39**, 5429-5433 (2000).
- [20] T. Tsurumi, S. Ozawa, G. Abe, N. Ohashi, S. Wada, and M. Yamane, *Jpn. J. Appl. Phys.*, **39**, 5604-5608 (2000).
- [21] T. Iijima, H. Matsuda, Y. Hayashi and J. Onagawa, *Trans. Mat. Res. Soc. Japan*, **27**, 243-246 (2002).
- [22] Y. Yasuda, M. Akamatsu, M. Tani, M. Yoshida, K. Kondo, and T. Iijima, *Jpn. J. Appl. Phys.*, **40**, 5518-5522 (2001).

(Received October 11, 2003; Accepted March 10, 2004)